Articles

Molecular Recognition by *Escherichia coli* UDP-3-*O*-(*R*-3-hydroxymyristoyl)-*N*-acetylglucosamine Deacetylase Is Modulated by Bound Metal Ions†

Marcy Hernick and Carol A. Fierke*

Department of Chemistry, University of Michigan, Ann Arbor, Michigan 48109

Received August 10, 2006; Revised Manuscript Received October 12, 2006

ABSTRACT: The metal-dependent enzyme UDP-3-*O*-(*R*-3-hydroxymyristoyl)-*N*-acetylglucosamine deacetylase (LpxC) catalyzes the conversion of UDP-3-*O*-(*R*-3-hydroxymyristoyl)-*N*-acetylglucosamine to UDP-3-*O*-(*R*-3-hydroxymyristoyl)glucosamine and acetate. This is the committed step in the biosynthesis of lipid A, and for this reason, LpxC is a target for the development of antibiotics in the treatment of Gram-negative bacterial infections. Here we examine the importance of bound metal ion(s) and fatty acids for molecular recognition of ligands by LpxC. The $K_D^{product}$ value increases >1000-fold with the loss of the hydroxymyristoyl moiety, indicating that the enhanced catalytic efficiency of substrates containing this acyl group is mainly due to increased binding affinity. New fluorescent binding assays for measuring the affinity of LpxC for fatty acids indicate that myristate binds to LpxC 10-fold less tightly than palmitate and that fatty acid affinity is only modestly dependent on pH. Furthermore, LpxC homologues from different species have similar affinities for fatty acids despite alterations in protein sequence. In contrast, the affinity of LpxC for both product and fatty acids is significantly influenced (≤40-fold) by changes in the number and identity of metal ions bound to the LpxC active site. Therefore, interactions with these metal ions are critical for molecular recognition of ligands by LpxC and may mimic similar contacts with active site inhibitors. These data indicate that the potency of LpxC inhibitors in vitro can be altered by assay conditions used in screening and/or development of LpxC inhibitors and that the metal ion status of LpxC in vivo will likely influence the effectiveness of LpxC inhibitors as antibiotics.

Pathogenic Gram-negative bacteria, including *Pseudomonas aeruginosa*, *Escherichia coli*, *Klebsiella* sp., and *Enterococcus* sp., are responsible for approximately half of the serious human infections, and complications from Gram-negative sepsis account for ∼100000 deaths/year in the United States alone (*1*−*3*). Gram-negative bacteria such as *P. aeruginosa* are responsible for the chronic pulmonary infections associated with cystic fibrosis (CF) (*4*, *5*), which is the leading cause of morbidity and mortality in CF patients. This finding highlights the need for more effective antibacterial agents for the treatment of Gram-negative bacterial infections. Treatment is complicated by the innate resistance of these pathogens, acquired multidrug resistance, and the limited number of effective antibiotics; therefore, new therapeutic alternatives, including drugs that act on new targets, are needed (*6*−*8*).

The innate resistance of Gram-negative bacteria is largely attributed to the outer membrane surrounding these organisms (*9*, *10*). Lipid A is the core of lipopolysaccharides (LPS)[1] that form the outer membranes of Gram-negative bacteria and is also the component of LPS responsible for stimulating the immune system in septic shock (*11*). Consequently, there is interest in the development of inhibitors of lipid A biosynthesis as both antibiotics and antiendotoxins (*11*−*13*). Recently, several Gram-negative bacteria have been identified for their potential as bioterror agents and are listed as NIAID category A and B priority pathogens (including *Yersinia pestis*, *Francisella tularensis*, *Coxiella burnetti*, *Brucella* sp., *Burkholderia mallei*, *Rickettsia prowazekii*, *Salmonella* sp., and *Campylobacter jejuni*), further increasing the urgency for developing new antibiotics effective against these organisms (*14*).

† This work was supported by the National Institutes of Health (Grant GM40602 to C.A.F.) and the Cystic Fibrosis Foundation (Grant HERNIC05F0 to M.H.).

* To whom correspondence should be addressed. Phone: (734) 936-2678. Fax: (734) 647-4865. E-mail: fierke@umich.edu.

[1] Abbreviations: LPS, lipopolysaccharide; LpxC, UDP-3-*O*-(*R*-3-hydroxymyristoyl)-*N*-acetylglucosamine deacetylase; UDPGlcNAc, uridine-5′-diphosphate *N*-acetylglucosamine; myrUDPGlcNAc, UDP-3-*O*-(*R*-3-hydroxymyristoyl)-*N*-acetylglucosamine; myrUDPGlcNH$_2$, UDP-3-*O*-(*R*-3-hydroxymyristoyl)glucosamine; EcLpxC, *Escherichia coli* LpxC; AaLpxc, *Aquifex aeolicus* LpxC; BSA, bovine serum albumin; TCEP, tris(carboxyethyl)phosphine; EGTA, ethylene glycol bis(2-aminoethyl ether)-*N*,*N*,*N*′,*N*′-tetraacetic acid; GABC, general acid−base catalyst; BODIPY 500/510 C$_4$, C$_9$, 5-butyl-4,4-difluoro-4-bora-3a,4a-diaza-*s*-indacene-3-nonanoic acid; ADIFAB, acrylodated intestinal fatty acid binding protein.

10.1021/bi061625y CCC: $33.50
Published on Web 11/17/2006

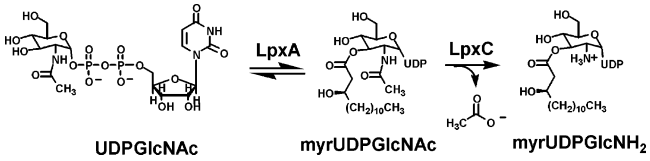

FIGURE 1: LpxC catalyzes the second step in the biosynthesis of lipid A.

UDP-3-*O*-(*R*-3-hydroxymyristoyl)-*N*-acetylglucosamine deacetylase (LpxC) is a metal-dependent enzyme that catalyzes the committed step in the biosynthesis of lipid A (Figure 1) (*15*). For this reason, LpxC is being pursued as a pharmaceutical target. The development of LpxC inhibitors as antimicrobial agents is attractive for the following reasons. Lipid A is essential for bacterial survival (*13*); the structure of LpxC is known (*16*−*19*), and there is past success in the development of inhibitors of metalloenzymes as drugs (*20*−*23*). Several LpxC inhibitors have been synthesized that contain a metal-chelating group (i.e., hydroxamate, phosphonate, carboxylate, thiol, or sulfonamide) that presumably binds to the active site metal ion (*20*, *24*−*28*). These inhibitors have antimicrobial activity against Gram-negative organisms, including *P. aeruginosa*, *Burkholderia cepacia*, and *Haemophilus influenza*, thus validating LpxC as a drug target (*20*, *24*−*28*). Interestingly, LpxC inhibitors display altered sensitivities to various bacterial strains which, at least in one case, is due to different molecular recognition properties of LpxC (*20*, *24*−*28*). Therefore, a comprehensive understanding of the molecular recognition properties of LpxC is warranted.

In particular, the potency of substrate analogue LpxC inhibitors against LpxC from *E. coli* and *Aquifex aeolicus* is differentially dependent on the length of the fatty acid chain (*25*). Furthermore, simple fatty acids bind to and inhibit LpxC, making these molecules good leads for the development of potent inhibitors (*16*, *19*). High-resolution structures of *A. aeolicus* LpxC that provide insights into the molecular basis for these findings have been determined (*16*−*19*). The overall topology of LpxC (Figure 2a) reveals a unique fold, consisting of two homologous domains each containing two α-helices sandwiched by a five-stranded *β*-sheet with the active site located at the interface of the two domains, as well as a previously unidentified zinc binding motif. Additionally, these structures reveal a hydrophobic tunnel [Figure 2B (*16*)] that leads through the enzyme to the active site of LpxC and forms a majority of the fatty acid binding site. This tunnel presumably contributes to the recognition of fatty acids by LpxC, leading to high-affinity binding. Previously, site-directed mutagenesis and product binding studies have demonstrated that a number of active site side chains (e.g., E78, H265, and F192) significantly contribute to molecular recognition of UDP-3-*O*-(*R*-3-hydroxymyristoyl)-GlcNH$_2$ by LpxC (*29*).

Herein, we analyze the contribution of bound metal ions and fatty acids to molecular recognition by *E. coli* LpxC. The hydroxymyristoyl moiety enhances the affinity of the product UDP-3-*O*-(*R*-3-hydroxymyristoyl)glucosamine (myrUDPGlcNH$_2$) more than 1000-fold, indicating that the enhanced catalytic efficiency of substrates containing this fatty acyl group is mainly due to enhanced binding affinity. To further examine molecular recognition of fatty acyl groups by LpxC, we developed two fluorescent binding assays that

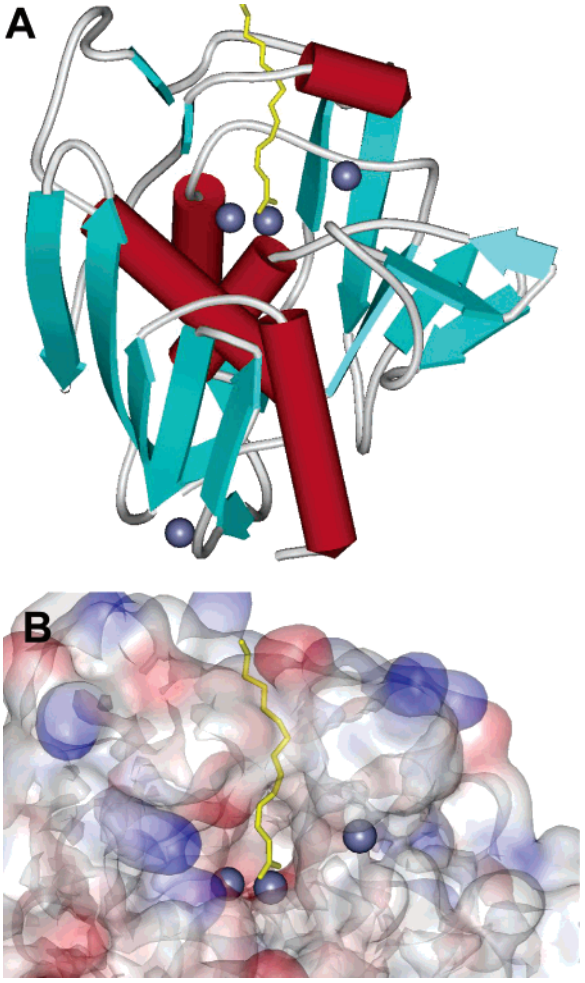

FIGURE 2: (A) Ribbon structure of zinc-inhibited *A. aeolicus* LpxC complexed with palmitate (yellow). Gray spheres represent zinc ions. (B) Hydrophobic tunnel that leads to the active site of LpxC [PDB entry 1P42 (*16*)].

either directly measure the affinity of the fluorescent fatty acid analogue 5-butyl-4,4-difluoro-4-bora-3a,4a-diaza-*s*-indacene-3-nonanoic acid (BODIPY 500/510 C$_4$, C$_9$) for LpxC or measure the affinity of unlabeled fatty acids for LpxC by competition with the fluorescent fatty acid binding protein ADIFAB. Using these assays, we demonstrate that myristate binds to LpxC 10-fold less tightly than palmitate, and with a comparable affinity to the BODIPY fatty acid, suggesting that fatty acid affinity correlates with chain length. Furthermore, the affinity of LpxC for fatty acids is only modestly dependent on pH, unlike the large pH dependence observed for binding of the product to LpxC (*29*). Deletion of side chains in the UDPGlcNAc binding site modestly enhances fatty acid affinity, while the largest effects on fatty acid affinity are observed upon alteration of the number and identity of metal ions at the active site of LpxC. Therefore, interactions with these metal ions are critical for molecular recognition of fatty acids by LpxC and may mimic similar contacts with active site inhibitors. These studies highlight features of the active site of LpxC that are critical for molecular recognition of fatty acids and may provide insights that will be useful for the development of potent and specific LpxC inhibitors.

MATERIALS AND METHODS

Mutagenesis and Protein Expression. The mutant plasmids were prepared using the Quik-change site-directed mutagenesis kit (Stratagene), and mutant LpxC proteins were overexpressed and purified as described previously (*29*). The apo- and stoichiometric Zn(II)−LpxC enzymes were prepared as previously described (*18*, *30*).

LpxC Deacetylase Assay. [^{14}C]UDP-3-*O*-(*R*-hydroxymyristoyl)-*N*-acetylglucosamine was prepared and the deacetylase activity measured as previously described (*18*, *30*, *31*). Briefly, assay mixtures containing 20 mM bis-tris propane (pH 7.5), bovine serum albumin (BSA, fatty acid free, 1 mg/mL), triscarboxyethylphosphine (TCEP, 0.5 mM), and [^{14}C]UDP-3-*O*-(*R*-hydroxymyristoyl)-*N*-acetylglucosamine or [^{14}C]UDP-3-*N*-acetylglucosamine were pre-equilibrated at 30 °C, and reactions were initiated by the addition of enzyme. After incubation for various times, the reaction was quenched by the addition of sodium hydroxide, which also cleaves the myristate substituent for ease of separation. Substrate and product were separated on PEI-cellulose TLC plates (0.1 M guanidinium HCl) and quantified by scintillation counting. Initial linear rates of product formation (< 20% reaction) were determined from these data, and rates were normalized to the concentration of enzyme and substrate in the assays to yield k_{cat}/K_M (μM^{-1} min^{-1}) values.

Determination of K_D Values of UDPGlcNH$_2$ Analogues. Dissociation constants (K_D) of [^{14}C]UDP-3-*O*-(*R*-3-hydroxymyristoyl)glucosamine and [^{14}C]UDP-glucosamine (Perkin Elmer) from an EcLpxC complex were measured using ultrafiltration (*29*). The concentration of product was held constant (below the K_D value, ≤73 nM), and the concentration of enzyme was varied (from 0 to 219 μM). Enzyme and substrate were incubated at 30 °C for 15−30 min to allow for product formation and ligand equilibration. Assay mixtures were then transferred into ultrafiltration devices (Microcons MWCO 30K); free and bound products were separated, and the amount of unbound (filtrate) and total product (retentate) was quantified using scintillation counting as previously described (*29*). The EP/P_{total} ratio was determined as a function of $[E]_{total}$, and K_D values were obtained by fitting eq 1 to these data. UDPGlcNH$_2$ binds very weakly to EcLpxC; therefore, a fixed EP of 0.9 (EP measured for myrUDPGlcNH$_2$) was used to estimate UDPGlcNH$_2$ affinity.

$$\frac{EP}{P_{total}} = \frac{(EP/P_{total})_{Endpt}}{1 + \frac{K_D}{E_{total}}} + (EP/P_{total})_{Background} \quad (1)$$

$K_D^{fatty\ acid}$ Determination Using a Competition-Based Assay. The K_D values of the fatty acids palmitate and myristate (Figure 3) for EcLpxC were determined using a competition-based assay with the fluorescent fatty acid binding protein ADIFAB (Invitrogen). ADIFAB is a fatty acid binding protein that is fluorescently labeled with acrylodan and can be used to detect free fatty acids by monitoring changes in fluorescence indicating the fraction of ADIFAB with bound fatty acid (*32*, *33*). First, the affinity of ADIFAB for fatty acids of interest was determined by titrating palmitate, myristate, or β-hydroxymyristate (0−30 μM) into a solution containing 0.2 μM ADIFAB [with 50 mM Tris, 1 mM EGTA, and 0.05% azide (pH 8.0)], and the resulting

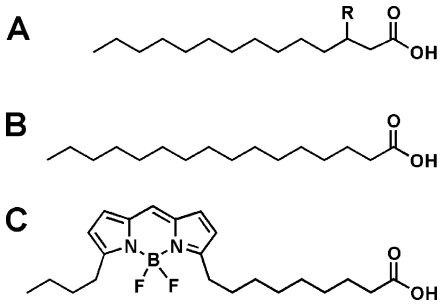

FIGURE 3: Structures of fatty acids: (A) myristic acid (R = H) and hydroxymyristic acid (R = OH), (B) palmitic acid, and (C) BODIPY C_4, C_9 fatty acid.

fluorescence emission intensity ratios (505/432) were measured following excitation at 390 nm and 30 °C. The K_D^{ADIFAB} values for palmitate, myristate, and β-hydroxymyristate dissociating from ADIFAB were determined to be 0.8, 3.3, and >20 μM, respectively, using the logarithmic form of eq 2 as described in the Invitrogen protocol

$$[FFA] = K_D Q \frac{R - R_o}{R_{max} - R} \quad (2)$$

where R represents the F_{505}/F_{432} ratio with R_o and R_{max} referring to the fully unbound and bound species, respectively, and Q represents the ratio of F_o/F_{max} at 432 nm. Saturation values (R_{max} = 11.5 and Q = 19) are provided in the Invitrogen protocol and were used for these calculations.

The $K_D^{fatty\ acid}$ values for EcLpxC were determined by premixing ADIFAB (0.2 μM) and fatty acid (3 μM palmitate or 7 μM myristate) to form the ADIFAB FA complex in 50 mM Tris, 1 mM EGTA, and 0.05% azide (pH 8.0), titrating EcLpxC (from 0 to 100 μM) into the solution, and measuring changes in the fluorescence emission ratio (505/432) at 30 °C. As the free fatty acid binds to EcLpxC, bound fatty acid dissociates from the ADIFAB·fatty acid complex to re-establish the equilibrium and a decrease in F_{505}/F_{432} is observed. The $K_D^{fatty\ acid}$ values for EcLpxC were determined by fitting eq 3 to the decrease in F_{505}/F_{432} using the K_D^{ADIFAB} values measured above, and an end point of 0.27 (experimentally determined F_{505}/F_{432} value for ADIFAB only).

$$\frac{ADIFAB{\cdot}FA}{FA_{total}} = \frac{(ADIFAB{\cdot}FA/FA_{total})_{\Delta}}{1 + \frac{K_D^{LpxC}}{[LpxC]}\left(1 + \frac{[FA]}{K_D^{ADIFAB}}\right)} + (ADIFAB{\cdot}FA/FA_{total})_{Initial} \quad (3)$$

Determination of $K_D^{fatty\ acid}$ Using Ultrafiltration. The dissociation constant (K_D value) of the fatty acid analogue 5-butyl-4,4-difluoro-4-bora-3a,4a-diaza-*s*-indacene-3-nonanoic acid [BODIPY 500/510 C_4, C_9, Molecular Probes (Figure 3)] for EcLpxC was measured using ultrafiltration (*29*). In these experiments, the concentration of fatty acid was held constant (0.6 μM) and the concentration of enzyme was varied (from 0 to 210 μM). Assay mixtures were transferred into ultrafiltration devices (microcons MWCO 30K), and the free and bound fatty acid were separated by centrifuging the samples at 3000 rpm for 2.5 min. An equal volume of filtrate and retentate was removed and diluted 13-fold into 6 M urea to denature LpxC, and the amount of fatty acid in each fraction was quantified using fluorescence intensity measure-

ments (excitation at 480 nm, emission at 516 nm). The concentration of bound fatty acid was calculated from the difference between the two samples, and K_D values were obtained by fitting eq 4 to the dependence of $E{\cdot}FA/FA_{total}$ on $[E]_{total}$.

$$\frac{E{\cdot}FA}{FA_{total}} = \frac{(E{\cdot}FA/FA_{total})_{Endpoint}}{1 + \frac{K_D}{E_{total}}} + FL_{Bkgd} \quad (4)$$

$K_D^{fatty\ acid}$ Determination Using Fluorescence Anisotropy Measurements. The K_D value of BODIPY fatty acid for EcLpxC was also determined using anisotropy measurements. The concentration of BODIPY fatty acid was held constant [0.1 μM, in 25 mM HEPES and 1.5 mM TCEP (pH 7.5)], and increasing concentrations of enzyme (from 0 to 210 μM) were titrated into the solution at 30 °C. Fluorescence anisotropy (excitation at 480 nm, emission at 516 nm) was measured ~3 min after each addition of EcLpxC, and K_D values were determined by fitting eq 4 to these data. End points typically ranged from 0.28 to 0.30 for these experiments. When the fatty acid affinity decreases significantly, the end point cannot be adequately fit; in this case, the end point value obtained for the H19Q mutant (0.29) was used. To determine if ionizations were important for binding of fatty acid to LpxC, K_D values were determined for EcH19Q and EcE78A at various pH values (25 mM buffer and 1.5 mM TCEP at pH *x*, MES at pH 5−6.5, and bis-tris propane at pH 7−9.8), and the pK_a values were determined by fitting eq 5 to these data.

$$K_{D,app} = K_{D1}\left[1/\left(1 + \frac{K_a}{H}\right)\right] + K_{D2}\left[1/\left(1 + \frac{H}{K_a}\right)\right] \quad (5)$$

To examine the effect of metal ions on fatty acid affinity, $K_D^{fatty\ acid}$ values were measured in the presence of either 100 μM $CaCl_2$, $CdCl_2$, $CoSO_4$, $CuSO_4$, $FeCl_2$, $MgSO_4$, $MnCl_2$, $NiSO_4$, or $ZnSO_4$ in the assay buffer. Higher concentrations of metal ions result in precipitation of LpxC. The $K_D^{fatty\ acid}$ was determined as a function of Zn(II) concentration for H19Q LpxC at pH 7.5, and these data suggest that the K_D^{Zn} for the inhibitory site is ~11 μM (data not shown); therefore, $Zn(II)_2$-inhibited LpxC predominates at 100 μM Zn(II).

RESULTS

Contribution of the Fatty Acid Moiety to the Affinity of the Product for EcLpxC. Understanding the features that govern molecular recognition will provide valuable information for the optimization of LpxC inhibitors. In particular, identification of specific groups that provide important contacts can be used to direct the modification of lead compounds to provide inhibitors with enhanced potency and specificity. The UDP moiety of the $myrUDPGlcNH_2$ product has previously been shown to contribute ~2.9 kcal/mol to the overall binding affinity (8.0 kcal/mol) of product for EcLpxC (*29*). To complement these studies, we have examined the importance of the myristoyl moiety to molecular recognition by EcLpxC. Measurements of the steady state turnover of deacetylation catalyzed by EcLpxC show that the value of k_{cat}/K_M for UDPGlcNAc is decreased from 460 to 0.026 min^{-1} μM^{-1} (1.8×10^4-fold decrease) at pH 7.5 compared to that of myrUDPGlcNAc, demonstrating that the fatty acid moiety is essential for high catalytic efficiency. Previously, a 5×10^6-fold decrease in activity was observed using UDPGlcNAc as a substrate at pH 5.5 (*30*). To ascertain the importance of the fatty acid moiety for binding of ligand to EcLpxC, the binding affinity of UDPGlcNAc was analyzed by ultrafiltration; less than 7% of the UDPGlcNAc binds to 100 μM EcLpxC, indicating that the $K_D \geq 1.5$ mM (Figure 4). Since the $K_D^{Product}$ value is 1.5 μM (*29*), the hydroxymyristoyl group increases the affinity of the product to EcLpxC by >1000-fold. Therefore, decreased binding affinity caused by loss of interactions with the fatty acyl group is sufficient to explain the majority of the observed decrease in catalytic efficiency of LpxC for deacetylation of UDPGlcNAc compared to myrUDPGlcNAc.

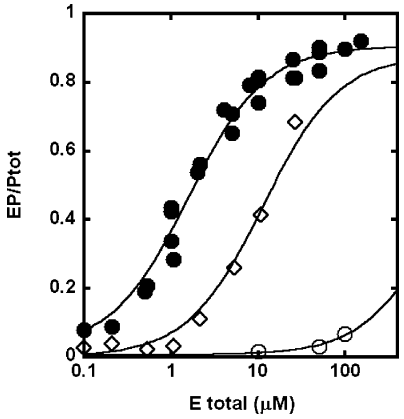

FIGURE 4: Product binding EcLpxC. The binding of (●) $myrUDPGlcNH_2$ and (○) $UDPGlcNH_2$ to the Zn−EcLpxC complex and (◇) $myrUDPGlcNH_2$ to the zinc-inhibited Zn_2−EcLpxC complex was assessed in 25 mM HEPES and 1.5 mM TCEP (pH 7.5), as described in Materials and Methods. The K_D values were obtained by fitting eq 1 to the resulting data.

Binding of Fatty Acid to EcLpxC. The data given above demonstrate that the fatty acid moiety is critical for molecular recognition by LpxC. To further investigate the determinants of fatty acid recognition by LpxC, we measured the K_D values of the fatty acids palmitate and myristate (structures shown in Figure 3) using a competition-based assay with the fluorescently labeled fatty acid binding protein ADIFAB as 4.2 ± 0.5 and 44 ± 2 μM, respectively (Figure 5). These data suggest that the binding affinity of LpxC for fatty acids increases with chain length, consistent with previous findings (*16*).

In addition, recognition of fatty acid by EcLpxC was directly probed using a fluorescent fatty acid analogue. The K_D value of a BODIPY fatty acid analogue (Figure 3) was determined using ultrafiltration experiments, where fatty acid binding was assessed by measuring the fluorescence intensity of separated bound and unbound fatty acid, and/or titration experiments where fatty acid binding was assessed directly by monitoring changes in anisotropy following addition of enzyme (Figure 6). Both approaches yield identical results for the affinity of EcLpxC for this fatty acid; therefore, anisotropy measurements were used for the remaining experiments. An additional advantage of this assay is that it is easily adapted to a 96-well format to screen for LpxC inhibitors (data not shown). We chose to vary the concentration of enzyme rather than fatty acid in these experiments since this both avoids micelle formation and leads to

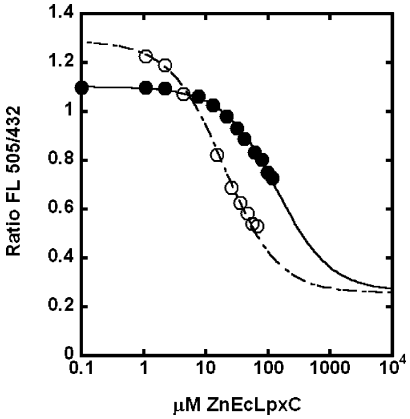

FIGURE 5: Fatty acid binding to EcLpxC. ADIFAB (0.2 μM) was premixed with (○) palmitate (3 μM) or (●) myristate (7 μM) in 50 mM Tris, 1 mM EGTA, and 0.05% azide (pH 8.0) at 30 °C to form the ADIFAB−FA complex. LpxC was titrated into the solution, and the changes in the fluorescence emission ratio (F_{505}/F_{432}) were determined, as described in Materials and Methods. The K_D values were obtained by fitting eq 3 to the resulting data.

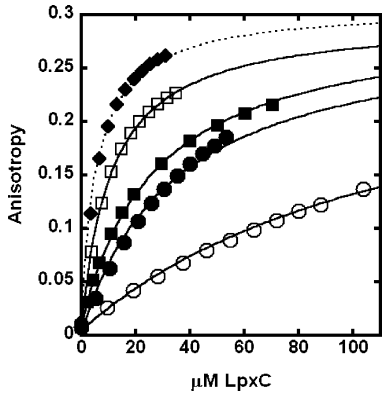

FIGURE 6: BODIPY fatty acid binding to (●) Zn WT, (○) Co WT, (■) apo WT, (□) H19Q, and (◆) H19Q with 78 mM UDPGlcNAc. The anisotropy of the BODIPY group (excitation at 480 nm, emission at 516 nm) was measured at 30 °C following the addition of LpxC to a solution of the BODIPY fatty acid (0.1 μM) in 25 mM HEPES and 1.5 mM TCEP (pH 7.5), as described in Materials and Methods. The K_D values were obtained by fitting eq 4 to the resulting data.

Table 1: $K_D^{\text{BODIPY fatty acid}}$ Values for Mutations that Significantly Affect the Affinity of EcLpxC

E. coli LpxC[a,b]	K_D (μM)[c] for E·M_A	K_D (μM)[d] for E·Zn_A·Zn_B
Zn^{2+} WT	37 ± 2	7 ± 0.3
Co^{2+} WT	126 ± 5	–
H19Y	17 ± 1	2 ± 0.2
H19Q	11 ± 1	2 ± 0.1
F192A	87 ± 8	11 ± 1
D197E	44 ± 4	1.3 ± 0.2

[a] The K_D values for LpxC were determined at 30 °C [25 mM HEPES and 1.5 mM TCEP (pH 7.5)] using anisotropy measurements as described in Materials and Methods. [b] The K_D values for H19A, E78A, K143A, N162A, T191A, D197A, K239A, and H265A mutations changed ≤2-fold compared to that of WT LpxC (with or without Zn). [c] The metal-substituted enzymes were prepared with a metal stoichiometry of 1:1 as described in Materials and Methods. [d] The K_D values were determined in the presence of 100 μM $ZnSO_4$, leading to the E·Zn_2 form of LpxC.

the largest signal change. The BODIPY fatty acid analogue binds to EcLpxC with a K_D value of 37 μM (Table 1), consistent with previous low micromolar affinities measured for fatty acids binding to *A. aeolicus* LpxC (*16*). The finding

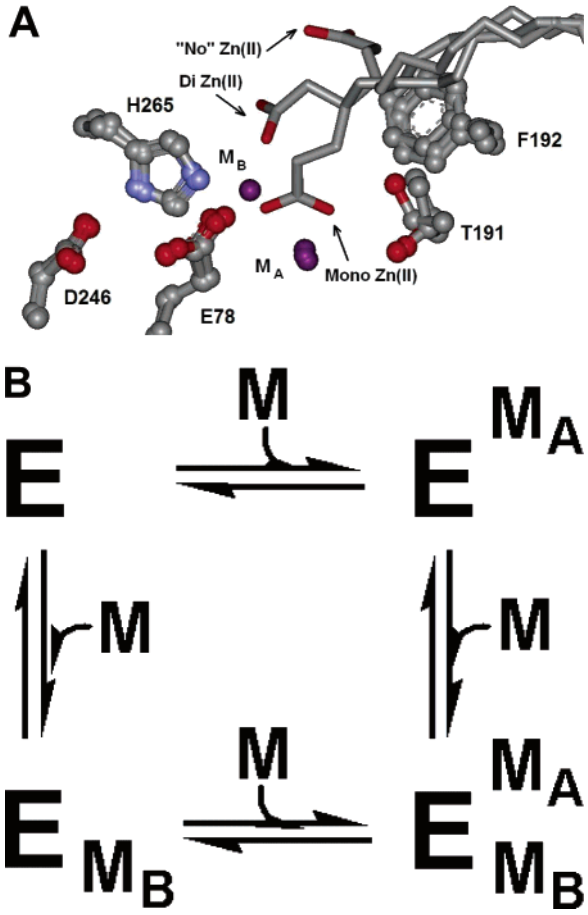

FIGURE 7: (A) Overlay of alternative conformations of palmitate coordinated to *A. aquifex* "apo" LpxC (PDB entry 1YHC), the catalytic Zn(II)−LpxC complex (PDB entry 1YH8), and the inhibited $Zn(II)_2$−LpxC complex (PDB entry 1P42) (*16*, *18*). (B) Possible metal−enzyme complexes that can bind fatty acid. M is the metal ion, E EcLpxC, M_A the catalytic site, and M_B the inhibitory site.

that EcLpxC has comparable affinities for the BODIPY fatty acid and myristate suggests that the BODIPY fatty acid is a good probe of the molecular recognition of fatty acids by LpxC. The addition of a subsaturating UDPGlcNAc concentration (20−80 mM, Figure 6) modestly enhances the fatty acid affinity (~1.5-fold), suggesting that there is binding synergy between the two portions of the LpxC product myrUDPGlcNH$_2$.

Role of the Metal Ion in Product and Fatty Acid Binding. Inhibitors of metalloproteins, including LpxC, rely on the incorporation of a metal chelating group to target the catalytic metal ion (M_A) (Figure 7) for activity and specificity. Consequently, the contribution of the metal ion to ligand affinity and molecular recognition is important for LpxC inhibitors. Substitution of the active site Zn(II) (Zn_A) with Co(II) enhances product affinity of EcLpxC by 2-fold, suggesting that the identity of the active site metal ion influences product recognition by LpxC (*29*). To further examine the role of active site metal ions in product affinity, we measured the effect of removing the zinc ion (apoenzyme) or of binding a second inhibitory Zn(II) (Zn_B), in forming an inactive binuclear LpxC·$Zn(II)_2$·myrUDPGlcNH$_2$ complex, on K_D^{Product}. The apoenzyme binds myrUDPGlcNH$_2$ with an affinity (1.5 ± 0.5 μM) comparable to that of the Zn·LpxC complex, while the inhibitory zinc ion diminishes

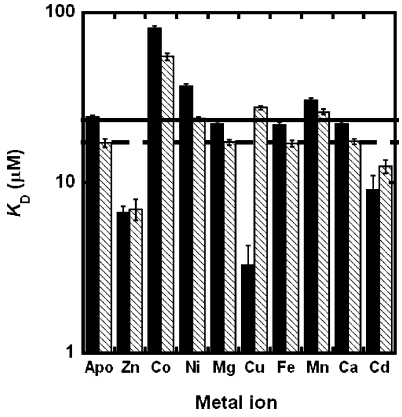

FIGURE 8: Effects of metal ions on the affinity of BODIPY fatty acid for EcLpxC (black bars) and EcC63A LpxC (hatched bars). The position of the lines indicates the expected affinity if the added metal ions have no effect on fatty acid affinity for WT (—) or EcC63A (– – –). The anisotropy of the BODIPY group (excitation at 480 nm, emission at 516 nm) was measured at 30 °C following the addition of LpxC (either WT or EcC63A) to a solution of the BODIPY fatty acid (0.1 μM) in 25 mM HEPES and 1.5 mM TCEP (pH 7.5) in the absence (apo) or presence of the indicated metal ions at 100 μM, as described in Materials and Methods. The K_D values were obtained by fitting eq 4 to the resulting data.

product affinity by ~8-fold (Figure 4), indicating that bound Zn_B leads to nonoptimal product affinity. In contrast, the addition of either 1 or 10 mM Mg(II) has no effect on the apparent dissociation constant for myrUDPGlcNH$_2$.

Crystal structures of LpxC complexes (*16*, *18*) indicate that the head group of bound palmitate exists in at least three conformations (Figure 7), coordinated to either the catalytic Zn(II) (M_A), the inhibitory Zn(II) (M_B), or neither. This finding suggests that interactions with metal ion(s) may contribute to fatty acid affinity and recognition by LpxC. Therefore, $K_D^{\text{fatty acid}}$ values for apo-LpxC and Zn_2-bound LpxC (inhibited, binuclear zinc site) were determined. These data indicate that the BODIPY fatty acid binds with highest affinity to the Zn_2·LpxC complex ($K_D = 6.7$ μM) followed by apo-LpxC ($K_D = 24$ μM), with the weakest affinity for the Zn·LpxC complex ($K_D = 37$ μM). These data indicate that metal carboxylate coordination and associated changes in the protein−fatty acid contacts are slightly unfavorable (1.5-fold) in the Zn·LpxC complex, while interactions with the inhibitory zinc are more favorable (5-fold).

We also investigated whether metal ion identity alters fatty acid recognition, by measuring the affinity of LpxC for BODIPY-FA in the presence of various divalent metal ions (Figure 8). Several divalent metal ions [i.e., Co(II), Ni(II), and Mn(II)] support catalytic activity in lieu of Zn(II), while others [notably Cu(II)] bind stoichiometrically to LpxC but do not activate the enzyme (*30*). The $K_D^{\text{fatty acid}}$ values were determined by titrating apo-LpxC into solutions containing the fatty acid and each metal ion at 100 μM. Under these conditions, there are several potential complexes, including E, E·M_A, E·M_B, or E·M_AM_B (Figure 7B), that could bind fatty acid. The binding data (Figure 8) demonstrate that Ca(II) and Mg(II) have no effect on the affinity of apo-LpxC for fatty acids, suggesting either that these metal ions do not bind to LpxC or that the metal−carboxylate interaction is extremely weak. An increase in the value of $K_D^{\text{fatty acid}}$ is observed following addition of the catalytically competent metal ions, Co(II), Ni(II), and Mn(II), indicating that these ions bind to LpxC and likely coordinate to the carboxylate group of the fatty acid, as observed for Zn(II) (Figure 7A), decreasing the fatty acid affinity compared to that of apo-EcLpxC. These K_D values do not significantly change (< 2-fold) when the concentration of metal ion is doubled (i.e., 200 μM), indicating that the observed effects on K_D arise from binding of fatty acid to an E·M complex. In contrast, there is a 3−8-fold enhancement of fatty acid affinity observed upon addition of Cd(II) and Cu(II) to apo-EcLpxC, indicating that these metal ions bind to LpxC and likely enhance the affinity by coordinating to the fatty acid, although neither Cd(II) or Cu(II) activates catalysis.

Since added metal ions could presumably bind at the catalytic site (M_A), the inhibitory site (M_B), or both sites (Figure 7), we also examined the $K_D^{\text{fatty acid}}$ values of the EcC63A LpxC mutant in the presence of 100 μM metal (Figure 8). In this mutant, one of the ligands for the inhibitory metal binding site [M_B; EcLpxC side chains of E78, H265, and C63 (unpublished results), and a water molecule] has been removed, significantly decreasing the affinity for metal ions at this site. For the majority of the metal ions that have been examined [Ca(II), Mg(II), Mn(II), Co(II), Ni(II), and Fe(III)], $K_D^{\text{fatty acid}}$ is altered < 2-fold relative to that of wild-type LpxC, suggesting that the inhibitory site either is not occupied or does not play an important role in molecular recognition of fatty acids for these metal ions. Therefore, the changes in fatty acid affinity observed for Co(II), Ni(II), and Mn(II) with wild-type (WT) EcLpxC are likely due to interaction with the metal ion bound at the catalytic site (M_A). In contrast, the affinity of the EcC63A mutant for the BODIPY fatty acid decreases 8- and 1.4-fold compared to that of WT LpxC in the presence of Cu(II) and Cd(II), respectively. These results suggest that the majority of the enhanced affinity of fatty acid for WT LpxC caused by the addition Cu(II), and possibly Cd(II), is due to interaction of the fatty acid with the metal ion at the inhibitory site (M_B), as previously observed for Zn(II).

Binding of Fatty Acid to LpxC from Other Sources. LpxC inhibitors display altered sensitivities to various bacterial strains (*20*, *24*−*28*), and measured inhibition constants depend on both the length of the fatty acyl chain and the species of enzyme. This suggests that molecular recognition of fatty acids may vary in homologues of LpxC from different sources. In fact, the affinity of apo-LpxC from both *A. aeolicus* and *P. aeruginosa* for the BODIPY fatty acid is decreased ~3-fold compared to that of EcLpxC. These data indicate that, in the absence of metal ions, the recognition properties of Aa, Ec, and Pa LpxC for simple fatty acid molecules are similar. Furthermore, as observed for EcLpxC, fatty acid affinity is enhanced 5−7-fold for AaLpxC and PaLpxC with the addition of 100 μM Zn(II). [These affinities may represent lower limits of $K_D^{\text{fatty acid}}$ as 100 μM Zn(II) may not saturate the inhibitory zinc site in AaLpxC and PaLpxC; these proteins precipitate at higher concentrations of Zn(II) (500 μM).] The similarities in the values of $K_D^{\text{fatty acid}}$ for LpxC from different sources indicate that recognition of longer fatty acids is comparable in these homologues.

pH Dependence of Binding of Fatty Acid to EcLpxC. The affinity of the fluorescent fatty acid for EcLpxC was determined as a function of pH using an LpxC mutant (H19Q) that binds the fluorescent fatty acid ~3-fold more

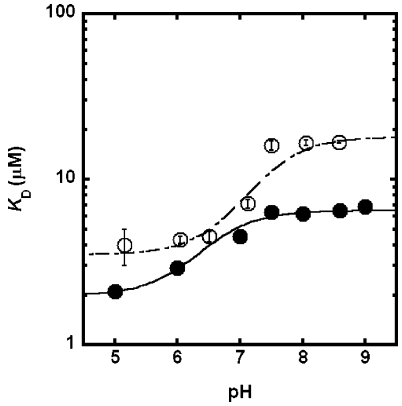

FIGURE 9: pH dependence of the affinity of BODIPY fatty acid for (●) EcH19Q and (○) EcE78A. The K_D values were measured at 30 °C by monitoring the anisotropy (excitation at 480 nm, emission at 516 nm) of the BODIPY fatty acid (0.1 μM), as described in Materials and Methods. The pK_a values of 6.6 ± 0.1 (H19Q) and 7.4 ± 0.1 (E78A) were obtained by fitting eq 5 to these data.

tightly than WT to enhance the accuracy of these experiments. These data (Figure 9) reveal that fatty acid binding is only modestly dependent on pH; a single ionization is observed in the value of $K_D^{\text{fatty acid}}$, reflecting a deprotonation that leads to a 2-fold decrease in affinity with a pK_a value of 6.6 ± 0.1. In contrast, a 180-fold change in affinity is observed in the affinity of myrUDPGlcNH$_2$ for EcLpxC over this pH range (*29*). It is likely that this pK_a reflects ionization of a group located in the LpxC active site, rather than a group located in the hydrophobic tunnel. The reported pK_a value for E78 is 6.5 ± 0.2 (*18*, *34*), and the E78 side chain is located within 2.5−3 Å of the palmitate head group; therefore, we probed whether ionization of this side chain is responsible for the observed pK_a value. For the E78A mutant, the single ionization is still observed, although the observed pK_a value is increased modestly (7.3 ± 0.3), and the change in affinity is larger (~6-fold), suggesting that the originally observed pK_a value of 6.6 ± 0.1 does not reflect ionization of E78.

Effects of Mutagenesis on Fatty Acid Binding Affinity. Crystal structures of LpxC·palmitate complexes (*16*, *18*) indicate that the head group of palmitate binds in the active site of LpxC (Figure 7) with a nearly symmetrical bidentate interaction with the catalytic Zn(II), with T191 donating a hydrogen bond to one of the oxygen atoms and E78 and H265 donating hydrogen bonds to the other oxygen atom (*18*). The side chain of D246 is present as part of a charge relay with H265 and therefore may position the H265 side chain. Additionally, the side chains of H19, T191, and F192 are at the base of the hydrophobic tunnel and positioned to interact with palmitate. Consequently, the side chains of these residues are located within 4 Å of palmitate and therefore may play a role in recognition of fatty acids by LpxC. To examine this possibility, we measured the K_D values of the BODIPY fatty acid for EcLpxC containing mutations to the side chains of H19, E78, K143, N162, T191, F192, D197, K239, D246, and H265 containing either a single bound Zn(II) ion or two bound Zn(II) ions (Table 1). Most of these mutations alter the affinity of LpxC for fatty acids ≤2-fold, implying that the majority of active site side chains do not directly contact the fatty acid and that the metal−carboxylate interaction is responsible for the majority of fatty acid recognition by the UDPGlcNAc binding site.

DISCUSSION

The Fatty Acid Moiety Is Critical for Molecular Recognition of Product by LpxC. The finding that myrUDPGlcNH$_2$ binds to EcLpxC ≥1000-fold more tightly than UDPGlcNH$_2$ indicates that the fatty acid moiety is crucial for molecular recognition by LpxC. Furthermore, the magnitude of this decrease in binding affinity mirrors the decrease in catalytic activity that is observed for UDPGlcNAc (~18000-fold), suggesting that the decreased catalytic activity is mainly due to weak substrate binding. These findings indicate that incorporation of groups capable of occupying the hydrophobic tunnel should lead to LpxC inhibitors with enhanced potency.

Molecular Recognition of Fatty Acids by EcLpxC. Palmitate binds to LpxC ~10-fold more tightly than myristate, consistent with the finding that longer fatty acids have higher affinities for LpxC (Figure 5) (*16*). Additionally, the fluorescent BODIPY fatty acid analogue binds to EcLpxC with a $K_D^{\text{fatty acid}}$ value (37 μM) that is comparable to the $K_D^{\text{fatty acid}}$ value for myristate (44 μM), suggesting that it can be used as a probe for fatty acid recognition by LpxC. The K_D value of myristate is 80-fold weaker than K_D^{product} [1.5 ± 0.2 μM (*29*)] under similar conditions, indicating that the fatty acid moiety contributes a majority of the energy for binding of product to LpxC (4−6 kcal/mol out of 8 kcal/mol). Furthermore, the addition of UDPGlcNH$_2$ leads to a modest enhancement in fatty acid affinity, indicating synergy between the two regions of the product. These findings confirm the importance of the hydrophobic tunnel for recognition of ligands by LpxC.

LpxC inhibitors display altered sensitivities to various bacterial strains (*20*, *24*−*28*), implying that there may be different recognition properties for the various LpxC enzymes. However, the affinity of LpxC enzymes from different species for BODIPY fatty acid affinity varies ≤3-fold, suggesting either that LpxC enzymes from different Gram-negative bacteria do not recognize fatty acids differentially, despite the differences in sequence, or that the differences in binding are only apparent with shorter fatty acids. These results suggest that targeting the hydrophobic tunnel should lead to broad spectrum LpxC inhibitors; other regions of the active may need to be targeted for species-specific inhibitors.

The Metal Ion Status of LpxC Modulates the Affinity of both Product and Fatty Acid. Here we demonstrate that the affinity of a ligand for LpxC is dependent on both the number and identity of active site metal ions and is a general feature of molecular recognition used by LpxC. Previous work has shown that the affinity of product for LpxC is dependent on the identity of the catalytic metal ion (*29*). Here we show that addition of high Zn(II) decreases product affinity (Figure 4), indicating that binding of product to the Zn_2·LpxC complex is nonoptimal. The weakened product affinity is likely due to the fact that H265 is a ligand for the inhibitory Zn(II); interaction with H265 significantly enhances product affinity (*29*). Therefore, upon binding Zn_B, H265 becomes unavailable to interact with product. These results demonstrate that both the identity and number of active site metal ions influence product binding affinity.

Similarly, the fatty acid affinity of LpxC is dependent on the number of metal ions bound to the active site, increasing 5−7-fold as the number of bound Zn ions increases from zero to two for LpxC from *E. coli*, *P. aeruginosa*, and *A. aquifex.* These changes in fatty acid affinity with varying numbers of active site Zn(II) ions are likely attributed to the multiple conformations adopted by the bound fatty acids (Figure 7). Structural data indicate that palmitate binds to LpxC with a bidentate interaction with the catalytic metal ion and a monodentate interaction with the inhibitory zinc (*16*, *18*). Typical Zn(II)−carboxylate dissociation constants in small molecules range from 50 to 100 mM (*35*). However, in LpxC, addition of metal ions increases fatty acid affinity only ∼4-fold, which is less than the value of 10−20-fold predicted from known metal−carboxylate interactions, suggesting that the carboxylate−metal coordination is nonoptimal.

The identity of the active site metal ion significantly alters (up to 40-fold) $K_D^{\text{fatty acid}}$. Metal ions that do not bind to LpxC should not alter affinity, and consequently, the $K_D^{\text{fatty acid}}$ values measured in the presence of these metal ions will be identical to the apo-LpxC $K_D^{\text{fatty acid}}$ values for both WT and EcC63A. This trend is observed for Ca(II), Mg(II), and Fe(III), suggesting that these metal ions do not bind, or bind very weakly, to LpxC. This finding is not surprising given that these ions do not activate catalysis. All other metal ions that were probed alter the $K_D^{\text{fatty acid}}$ values relative to that of apo-LpxC, indicating that these metal ions bind to LpxC and influence fatty acid affinity.

To decipher whether the altered fatty acid binding observed for WT in the presence of a given metal ion is a result of metal ion binding at the catalytic site (M_A) or inhibitory site (M_B), $K_D^{\text{fatty acid}}$ values for WT and EcC63A were compared (Figure 7). (The EcC63A mutant binds the BODIPY fatty acid analogue ∼30% more tightly than WT; therefore, slightly lower $K_D^{\text{fatty acid}}$ values are observed.) Since Cys63 is not a metal ligand for the catalytic site, comparable $K_D^{\text{fatty acid}}$ values for WT and EcC63A are predicted for metal ions that bind preferentially to the catalytic site (M_A). The metal ions Co(II), Mn(II), and Ni(II) all exhibit this behavior. Preferential binding of these metal ions to the catalytic site (M_A) is also supported by the fact that all of these metal ions activate, but do not inhibit, catalytic activity (*30*). For metal ions that enhance fatty acid affinity through binding to the inhibitory site (M_B), the metal-dependent fatty acid affinity should decrease (K_D increase) in the Ec63A mutant compared to that of WT EcLpxC. This behavior is observed for Cu(II), Zn(II), and Cd(II), suggesting these ions bind to the inhibitory site (M_B) of LpxC. This result is consistent with the metal activation data which show Zn(II) inhibits LpxC at high concentrations and Cu(II) and Cd(II) do not activate catalysis even though Cu(II) binds to the enzyme (*30*). Interestingly, metal ions that bind preferentially at the M_A site tend to diminish fatty acid affinity, whereas metal ions that bind to the M_B site enhance affinity. Although the physiological importance of this finding is currently unknown, these data highlight the need to understand the active site metal ion status for the development of potent LpxC inhibitors.

Implications. In summary, these data demonstrate that fatty acids and bound metal ion(s) provide critical interactions that contribute to molecular recognition by LpxC and highlight the need to understand the active site metal ion status in vitro and in vivo for both evaluating enzyme activity and developing potent LpxC inhibitors. It is likely that metal ions will similarly influence inhibitor recognition, as all reported inhibitors target and presumably directly coordinate to the catalytic metal ion (M_A). Furthermore, the metal ion status of LpxC in vivo will influence inhibitor potency and sensitivity and, consequently, impact the effectiveness of LpxC inhibitors as antibiotics. Therefore, the concentrations of divalent metal ions [in particular Zn(II) and Cu(II)] used in LpxC inhibitor screens should be controlled for and should mimic in vivo metal concentrations. Physiologically, it is unlikely that Zn(II)-inhibited LpxC will be present to any significant extent as the inhibitory Zn(II) has a weak affinity for LpxC (K_{Zn} in the micromolar range), and the intracellular concentration of free Zn(II) is low [$[Zn]_{free} \leq 1 \times 10^{-11}$ M (*36*, *37*)]. However, the ratio of mononuclear Zn(II)-bound LpxC to LpxC containing other divalent metal ions present in Gram-negative bacteria is likely to influence the effectiveness of LpxC inhibitors as antibacterial agents.

REFERENCES

1. Parillo, J. E. (1993) Pathogenic mechanisms of septic shock, *N. Engl. J. Med. 328*, 1471−1477.
2. Moine, P., and Abraham, E. (2004) Immunomodulation and sepsis: Impact of the pathogen, *Shock 22*, 297−308.
3. World Health Organization (2002) Explore simplified antimicrobial regimens for the treatment of neonatal sepsis.
4. Lyczak, J. B., Cannon, C. L., and Pier, G. B. (2002) Lung Infections Associated with Cystic Fibrosis, *Clin. Microbiol. Rev. 15*, 194−222.
5. Ratjen, F., and Doring, G. (2003) Cystic fibrosis, *Lancet 361*, 681−689.
6. Hughes, D. (2003) Exploiting genomics, genetics and chemistry to combat antibiotic resistance, *Nat. Rev. Genet. 4*, 432−441.
7. Miesel, L., Greene, J., and Black, T. A. (2003) Genetic strategies for antibacterial drug discovery, *Nat. Rev. Genet. 4*, 442−456.
8. Chalker, A. F., and Lunsford, R. D. (2002) Rational identification of new antibacterial drug targets that are essential for viability using a genomics-based approach, *Pharmacol. Ther. 95*, 1−20.
9. McKeegan, K. S., Borges-Walmsley, M. I., and Walmsley, A. R. (2002) Microbial and viral drug resistance mechanisms, *Trends Microbiol. 10*, S8−S14.
10. Hogan, D., and Kolter, R. (2002) Why are bacteria refractory to antimicrobials? *Curr. Opin. Microbiol. 5*, 472−477.
11. Raetz, C. R. H., and Whitfield, C. (2002) Lipopolysaccharide endotoxins, *Annu. Rev. Biochem. 71*, 635−700.
12. Darveau, R. P. (1998) Lipid A diversity and the innate host response to bacterial infection, *Curr. Opin. Microbiol. 1*, 36−42.
13. Wyckoff, T. J. O., Raetz, C. R. H., and Jackman, J. E. (1998) Antibacterial and anti-inflammatory agents that target endotoxin, *Trends Microbiol. 6*, 154−159.
14. Roth, L. D., Khan, A. S., Lillibridge, S. R., Ostroff, S. M., and Hughes, J. M. (2002) Public health assessment of potential biological terrorism agents, *Emerging Infect. Dis. 8*, 225−230.
15. Anderson, M., Bull, H., Galloway, S., Kelly, T., Mohan, S., Radika, K., and Raetz, C. (1993) UDP-N-acetylglucosamine acyltransferase of *Escherichia coli*. The first step of endotoxin biosynthesis is thermodynamically unfavorable, *J. Biol. Chem. 268*, 19858−19865.
16. Whittington, D. A., Rusche, K. M., Shin, H., Fierke, C. A., and Christianson, D. W. (2003) Crystal structure of LpxC, a zinc-dependent deacetylase essential for endotoxin biosynthesis, *Proc. Natl. Acad. Sci. U.S.A. 100*, 8146−8150.
17. Coggins, B. E., Li, X. C., McClerren, A. L., Hindsgaul, O., Raetz, C. R. H., and Zhou, P. (2003) Structure of the LpxC deacetylase with a bound substrate-analog inhibitor, *Nat. Struct. Biol. 10*, 645−651.
18. Hernick, M., Gennadios, H. A., Whittington, D. A., Rusche, K. M., Christianson, D. W., and Fierke, C. A. (2005) UDP-3-O-((R)-3-hydroxymyristoyl)-N-acetylglucosamine deacetylase functions

through a general acid-base catalyst pair mechanism, *J. Biol. Chem. 280*, 16969−16978.
19. Coggins, B. E., McClerren, A. L., Jiang, L., Li, X., Rudolph, J., Hindsgaul, O., Raetz, C. R. H., and Zhou, P. (2005) Refined Solution Structure of the LpxC-TU-514 Complex and pKa Analysis of an Active Site Histidine: Insights into the Mechanism and Inhibitor Design, *Biochemistry 44*, 1114−1126.
20. White, R. J., Margolis, P. S., Trias, J., and Yuan, Z. Y. (2003) Targeting metalloenzymes: A strategy that works, *Curr. Opin. Pharmacol. 3*, 502−507.
21. Leung, D., Abbenante, G., and Fairlie, D. P. (2000) Protease inhibitors: Current status and future prospects, *J. Med. Chem. 43*, 305−341.
22. Supuran, C. T., Casini, A., and Scozzafava, A. (2003) Protease inhibitors of the sulfonamide type: Anticancer, antiinflammatory, and antiviral agents, *Med. Res. Rev. 23*, 535−558.
23. Supuran, C. T., Scozzafava, A., and Casini, A. (2003) Carbonic anhydrase inhibitors, *Med. Res. Rev. 23*, 146−189.
24. Onishi, H. R., Pelak, B. A., Gerckens, L. S., Silver, L. L., Kahan, F. M., Chen, M. H., Patchett, A. A., Galloway, S. M., Hyland, S. A., Anderson, M. S., and Raetz, C. R. H. (1996) Antibacterial agents that inhibit lipid A biosynthesis, *Science 274*, 980−982.
25. Jackman, J. E., Fierke, C. A., Tumey, L. N., Pirrung, M., Uchiyama, T., Tahir, S. H., Hindsgaul, O., and Raetz, C. R. H. (2000) Antibacterial agents that target lipid A biosynthesis in Gram-negative bacteria: Inhibition of diverse UDP-3-O-(R-3-hydroxymyristoyl)-N-acetyglucosamine deacetylases by substrate analogs containing zinc binding motifs, *J. Biol. Chem. 275*, 11002−11009.
26. Pirrung, M. C., Tumey, L. N., Raetz, C. R. H., Jackman, J. E., Snehalatha, K., McClerren, A. L., Fierke, C. A., Gantt, S. L., and Rusche, K. M. (2002) Inhibition of the antibacterial target UDP-(3-O-acyl)-N-acetylglucosamine deacetylase (LpxC): Isoxazoline zinc amidase inhibitors bearing diverse metal binding groups, *J. Med. Chem. 45*, 4359−4370.
27. Clements, J. M., Coignard, F., Johnson, I., Chandler, S., Palan, S., Waller, A., Wijkmans, J., and Hunter, M. G. (2002) Antibacterial activities and characterization of novel inhibitors of LpxC, *Antimicrob. Agents Chemother. 46*, 1793−1799.
28. Kline, T., Andersen, N. H., Harwood, E. A., Bowman, J., Malanda, A., Endsley, S., Erwin, A. L., Doyle, M., Fong, S., Harris, A. L., Mendelsohn, B., Mdluli, K., Raetz, C. R. H., Stover, C. K., Witte, P. R., Yabannavar, A., and Zhu, S. G. (2002) Potent, novel in vitro inhibitors of the *Pseudomonas aeruginosa* deacetylase LpxC, *J. Med. Chem. 45*, 3112−3129.
29. Hernick, M., and Fierke, C. A. (2006) Catalytic mechanism and molecular recognition of E. coli UDP-3-O-(R-3-hydroxymyristoyl)-N-acetylglucosamine deacetylase probed by mutagenesis, *Biochemistry*, in press.
30. Jackman, J. E., Raetz, C. R. H., and Fierke, C. A. (1999) UDP-3-O-(R-3-hydroxymyristoyl)-N-acetylglucosamine deacetylase of *Escherichia coli* is a zinc metalloenzyme, *Biochemistry 38*, 1902−1911.
31. Sorensen, P. G., Lutkenhaus, J., Young, K., Eveland, S. S., Anderson, M. S., and Raetz, C. R. H. (1996) Regulation of UDP-3-O-R-3-hydroxymyristoyl-N-acetylglucosamine deacetylase in *Escherichia coli*: The second enzymatic step of lipid a biosynthesis, *J. Biol. Chem. 271*, 25898−25905.
32. Richieri, G. V., Ogata, R. T., and Kleinfeld, A. M. (1992) A fluorescently labeled intestinal fatty acid binding protein. Interactions with fatty acids and its use in monitoring free fatty acids, *J. Biol. Chem. 267*, 23495−23501.
33. Richieri, G. V., Ogata, R. T., and Kleinfeld, A. M. (1994) Equilibrium constants for the binding of fatty acids with fatty acid-binding proteins from adipocyte, intestine, heart, and liver measured with the fluorescent probe ADIFAB, *J. Biol. Chem. 269*, 23918−23930.
34. McClerren, A. L., Zhou, P., Guan, Z., Raetz, C. R. H., and Rudolph, J. (2005) Kinetic Analysis of the Zinc-Dependent Deacetylase in the Lipid A Biosynthetic Pathway, *Biochemistry 44*, 1106−1113.
35. Smith, R. M., Martell, A. E., and Motekaitis, R. J. (2003) NIST Critically selected stability constants of metal complexes database. National Institute of Standards and Technology.
36. Bozym, R. A., Thompson, R. B., Stoddard, A. K., and Fierke, C. A. (2006) Measuring picomolar intracellular exchangeable zinc in PC-12 cells using a ratiometric fluorescence biosensor, *ACS Chem. Biol. 1*, 103−111.
37. Outten, C. E., and O'Halloran, T. V. (2001) Femtomolar sensitivity of metalloregulatory proteins controlling zinc homeostasis, *Science 292*, 2488−2492.

BI061625Y